



Network structure and electromechanical properties of viscose-graphene conductive yarn assemblies



HPSTAR
477-2017

Hui Ma ^a, Wen Wu ^a, Jianda Cao ^a, Binbin Yue ^{b, c}, Huanxia Zhang ^{a, *}

^a College of Material and Textile Engineering, Jiaying University, Jiaying, Zhejiang, 314001, PR China

^b Center for High Pressure Science and Technology Advanced Research, 1690 Cailun Rd, Pudong, Shanghai, 201203, China

^c Advanced Light Source, Lawrence Berkeley National Laboratory, Berkeley, CA, 94720, USA

ARTICLE INFO

Article history:

Received 17 September 2016

Received in revised form

22 December 2016

Accepted 23 December 2016

Available online 24 December 2016

Keywords:

Yarn assemblies

Graphene

Stitch structure

Electromechanical properties

ABSTRACT

Conductive yarns were successfully prepared through the assembly and reduction of graphene oxide on the surface of viscose yarns and the relationship between network structure of yarn assemblies and electromechanical properties of knitted or weave fabrics was analyzed. The loop and interlacing structure, which were provided by knitted and weave fabrics respectively, could result in different electrical properties under external stress because of the change of volume or contacting resistors of yarn assemblies. Herein, the stitch structure of fabrics was simulated as circuit model consisted of volume resistance or contact resistors. Based on such models and volume and contacting resistors of yarns, the simulated results agreed reasonably with the experimental data and major trends of both results were consistent. In addition, with the deformation of topology structure of fabrics under drawing, the fineness of yarns and densities of fabrics became changed, causing the increase or decrease of transfer rate of electrons along the yarns. The results provided a theory basis for the design and preparation of flexible conductive devices with the potential applications of energy storage/conversion, wearable sensor, transparent conducting films, flexible cell and so on.

© 2016 Elsevier Ltd. All rights reserved.

1. Introduction

During the past few decades, fibers made of carbon materials (carbon nanotubes or graphene) or coated with conductive materials have been used as flexible conductive devices with applications in energy storage/conversion, wearable sensor, flexible solar cells and so on [1–8]. Different conductive fibers, including carbon nanotube (CNT) fibers, graphene fibers, MnO₂/Zn₂SnO₄/carbon fibers, MnO₂/activated carbon fibers and so on, have been fabricated through wet spinning, dipping-drying treatments or roll-to-roll approach [9].

Some researchers have reported that neat CNT or graphene fibers could be fabricated through wet spinning and capable of making electrodes and solar cells [10–12]. The CNT fibers prepared by B. Vigolo et al., in 2000 exhibited excellent electrical conductivity (1000 S/m). Unlike the traditional strategies of continuous fibers built up from one-dimensional CNTs, C. Gao et al. first fabricated neat graphene fibers through the solution-based liquid

crystal phase spinning of graphene oxide solutions and followed by chemical reduction of HI solution. These graphene fibers showed an electrical conductivity of 2×10^4 S/m. The most promising applications of graphene fibers are mainly attributed to fiber/woven fabric supercapacitors.

X. Li et al. have fabricated the MnO₂/Zn₂SnO₄/carbon fibers hybrid composite by facile coating ultrathin films of MnO₂ to Zn₂SnO₄ nanowires grown on carbon fibers. The characteristics offer the excellent rate capability with specific energy of 36.8 Wh/kg and specific power of 32 kW/kg at density of 40 A/g respectively, and 1.2% loss of its initial specific capacitance after 1000 cycles. These composites are promising for next generation supercapacitors [13]. In addition, they have also fabricated highly conductive and flexible MnO₂/activated carbon fibers composites, and observed the excellent electrochemical performance of composites [14].

Among kinds of flexible conductive materials, the fibers coated with graphene through dipping, drying and reducing process have attracted attention because of higher conductive efficiency and better strain capacity under external force [15–19]. When these fibers make electrically conducting assemblies, excellent electrical

* Corresponding author.

E-mail address: zhuanghuanxia818@163.com (H. Zhang).

properties can be observed. Fabric electrodes with various distributions of resistors can be assembled, displaying different volume and contact resistance. In a fabric electrode, the whole resistance was found to be in parallel-series to the connection of contacting resistance of yarns, and for the single yarns, the resistance was a parallel connection of the volume resistance. When the fabric electrode was stressed, the topology of yarn assemblies and the appearance of the yarn in contact positions transformed, resulting in a change in volume and contacting resistors, until finally the whole resistance of the fabric decreased or increased, depending on stress direction. Thus, good understanding of the relationship between electromechanical properties and network structure of yarn assemblies is the key to the successful design and preparation of flexible conductive devices.

H. Zhang et al. have studied the electromechanical properties of knitted fabrics composed of carbon fibers using a model of weft plain knitting, and established a linear resistance-strain relationship. This relationship was influenced by loop network structure, and improved by series topology of fabrics, resulting in improvement of the sensitivity of the sensors. In addition, the resistance of the carbon fabric sharply decreased from about $3.5 \times 10^4 \Omega$ to about $1.2 \times 10^4 \Omega$ when the knitted fabrics has a maximum strain level at 20% due to the change of numbers of the contacting electrical resistors [20].

Besides the network structure of fiber assemblies, the deformation of fibers also affects the electrical resistance of resulting systems [21,22]. In our work, the electrical properties of viscose yarns with graphene coatings under tension were characterized and simulation models were established. Based on such models, the simulated equivalent resistance of fabrics could be calculated and were used to compare with the experimental data. In addition, the stitch structure of knitted and weave fabrics composed of conductive yarns was analyzed. Moreover, the relationship between electromechanical properties and stitch structure of both fabrics was also explored.

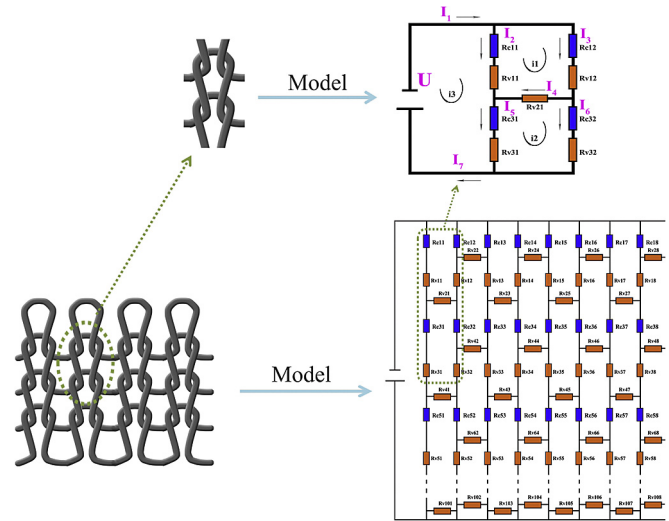


Fig. 1. The model of loops of knitted viscose fabrics. (A colour version of this figure can be viewed online.)

identical loops, whose equivalent resistance could be analyzed by Kirchhoff's law [24]. As shown in Fig. 1, each loop was made up of four contacting resistors (Rc) and five volume resistors (Rv), and such nine resistors formed three closed circuits.

The voltage of three closed circuits was calculated by the following Eq (1):

$$\begin{cases} I_3(RC_{12} + RV_{12}) + I_4RV_{21} - I_2(RC_{11} + RV_{11}) = 0 \\ I_6(RC_{32} + RV_{32}) - I_4RV_{21} - I_5(RC_{31} + RV_{31}) = 0 \\ I_2(RC_{11} + RV_{11}) + I_5(RC_{31} + RV_{31}) = U \end{cases} \quad (1)$$

Resistor matrix could then be calculated as:

$$Rx_{ij}^* = \begin{bmatrix} RC_{11} + RV_{11} + RC_{12} + RV_{12} + RV_{21} & -RV_{21} & -RC_{11} - RV_{11} \\ -RV_{21} & RV_{21} + RC_{32} + RV_{32} + RC_{31} + RV_{31} & -RC_{31} - RV_{31} \\ -RC_{11} - RV_{11} & -RC_{31} - RV_{31} & RC_{11} + RV_{11} + RC_{31} + RV_{31} \end{bmatrix} \quad (2)$$

2. Materials and methods

2.1. Model of knitted or weave fabrics

$$Rx_{ij}^* = \begin{bmatrix} RC_{11} + RV_{11} + RC_{12} + RV_{12} + RV_{21} & \dots & -RC_{11} - RV_{11} \\ \vdots & \ddots & \vdots \\ -RC_{11} - RV_{11} & \dots & RC_{11} + RV_{11} + RC_{31} + RV_{31} + \dots + RC_{n1} + RV_{n1} \end{bmatrix} \quad (3)$$

Viscose, which was regenerated from cellulose, had large deformation under stress due to breakage of hydrogen bonds between glucose chains and slippage of chains, resulting in a decrease of fiber cross-section [23]. In our work, unit resistivity of knitted or woven fabrics was composed of volume and contacting resistors, and two different models were built.

The stitch structure of knitted fabrics consisted of many

From Eq (2), Rc and Rv could be calculated, and finally, the resistivity of fabrics could be obtained according to the network structure of the fabrics (Fig. 1) and expressed as:

where n is odd.

In plain weave fabrics (Fig. 2), the stitch structure was different from that of knitted fabrics. Due to the presence of interlacing, the contact resistance was negligible, and the whole resistance of the fabric was related only to the volume resistance. According to these studies, H. Zhang et al. has established a model of electrical network and studied the electromechanical properties of polypyrrole-

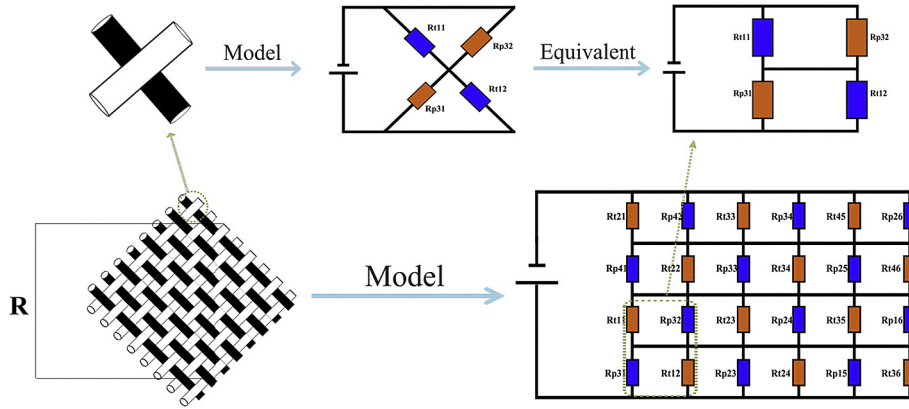


Fig. 2. The model of interlaced structure and weave fabrics. (A colour version of this figure can be viewed online.)

coated plain weave fabrics under uniaxial tension [25]. In our work, the electromechanical properties of weave fabrics composed of graphene-coated viscose yarns in diagonal direction were explored by combining theoretical and experimental analysis. Here, the volume resistor was divided into two sections according to warp and weft, and the resistance of warp and weft was simply represented by Rp and Rt respectively. An interlace point of warp and weft was considered as one unit, which included two Rp and two Rt.

The resultant resistance of three closed circuits could be obtained by the following Eq (4):

$$\begin{cases} (Rt_{12} + Rp_{31})i_1 - Rp_{31}i_3 = 0 \\ (Rt_{11} + Rp_{32})i_2 - Rt_{11}i_3 = 0 \\ -Rp_{31}i_1 - Rt_{11}i_2 + (Rp_{31} + Rt_{11})i_3 = U \end{cases} \quad (4)$$

Based on Eq (4), the resistance matrix could be calculated as:

$$R^* = \begin{bmatrix} Rt_{12} + Rp_{31} & 0 & -Rp_{31} \\ 0 & Rt_{11} + Rp_{32} & -Rt_{11} \\ -Rp_{31} & -Rt_{11} & Rp_{31} + Rt_{11} \end{bmatrix} \quad (5)$$

From Eq (5), Rp and Rt could be determined, and the resulting resistance of fabrics could be expressed as:

$$R^* = \begin{bmatrix} Rt_{21} + Rp_{42} & -Rp_{42} & 0 & 0 & 0 & 0 & \dots & -Rt_{21} \\ -Rp_{42} & Rt_{33} + Rp_{42} & -Rt_{33} & 0 & 0 & 0 & \dots & 0 \\ 0 & -Rt_{33} & Rt_{33} + Rp_{34} & -Rp_{34} & 0 & 0 & \dots & 0 \\ 0 & 0 & -Rp_{34} & Rt_{45} + Rp_{34} & -Rt_{45} & 0 & \dots & 0 \\ 0 & 0 & 0 & -Rt_{45} & Rt_{45} + Rp_{26} & -Rp_{26} & \dots & 0 \\ \vdots & \vdots & \vdots & \vdots & \vdots & \vdots & \ddots & \vdots \\ -Rt_{21} & 0 & 0 & 0 & 0 & 0 & \dots & Rt_{21} + Rp_{41} + Rt_{11} + Rp_{31} \end{bmatrix} \quad (6)$$

2.2. Materials and preparation

Commercial viscose yarns were kindly provided by Suzhou Shuishan Industrial Co., Ltd, Jiangsu. Before usage, sodium hydrate (NaOH) solutions were used to remove the oil impurities. Flake graphene and other reagents, including sulfuric acid (H₂SO₄, 98%), hydrogen peroxide (H₂O₂, 30%), hydrazine hydrate (N₂H₄·H₂O), sodium nitrate (NaNO₃) and potassium permanganate (KMnO₄) were all supplied by Sinopharm Chemical Reagent Co., Ltd.

For the preparation of reduced graphene oxide (RGO) coated viscose yarns, flake graphene was first treated to obtain graphene oxide (GO) according to the modified Hummer's method [26]. After that, GO coated viscose yarns (GO-VY) were prepared through dipping-drying treatments (twelve cycles) of GO dispersions on the viscose yarns. Then, RGO coated viscose yarns (RGO-VY) were prepared through the reducing treatment of GO-VY with the introduction of N₂H₄·H₂O solutions (3%). Finally, conductive knitted and woven fabrics could be obtained through the knitting or weaving of RGO-VY. In this manuscript, the amount (11.55%) of RGO onto the surface of yarns was calculated by TG curves of viscose fabric and RGO coated viscose fabric.

2.3. Characterization

A HITACHI S-4800 scanning electron microscope was used to characterize the morphology of the conductive fabrics using an acceleration voltage of 1 kV. Before characterization, fabric samples were coated with Au, employing an E1010 sputter coater (HITACHI, Japan). XPS measurements of viscose fabric, GO and GO coated viscose fabric were carried out on a spectrometer (XSAM800, Kratos, UK) operated at 1486.6 eV.

To evaluate electromechanical properties of conductive knitted

and woven fabrics, a three-dimensional video microscope system (KH-1300, HIROX, Japan) was used to record the change of stitch structure under stress. The tensile strength was recorded *in situ* by a 2715 materials testing machine for yarns and a 5566 materials testing machine for fabrics (Instron, America). The resistivity of yarns and fabrics was measured with a 2010 multimeter (Keithley, America) according to the International Electro Technical Commission 93–1980, which was similar with the method reported by some researchers [27].

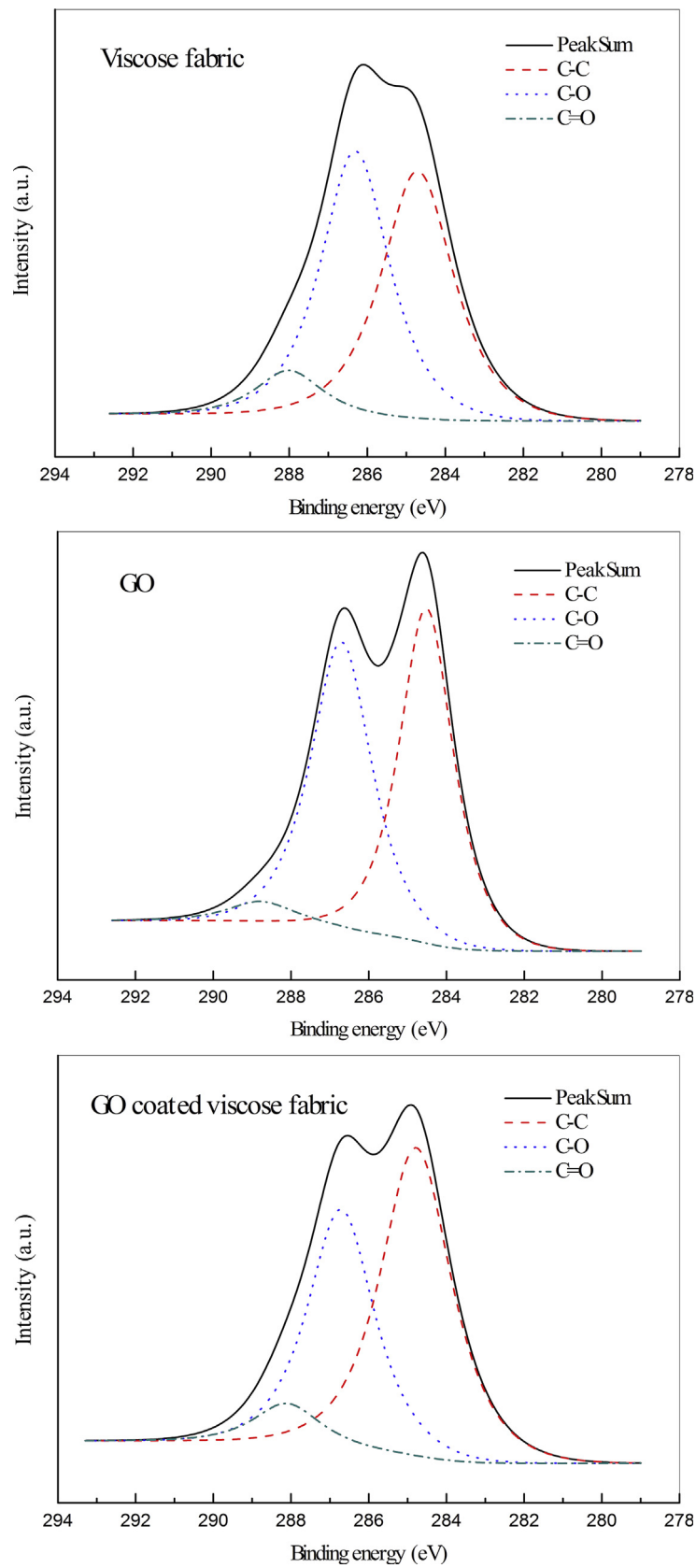


Fig. 3. XPS deconvoluted C1s component of viscose fabric, GO and GO coated viscose fabric.

Table 1

The related results summarized from XPS images.

Samples	C–C (at%) 284.6 eV	C–O (at%) 285.9 eV	C=O (at%) 287.1 eV
Viscose fabric	43.27	43.62	13.11
GO	45.80	6.61	47.59
GO coated viscose fabric	46.24	36.91	16.85

3. Results and discussion

3.1. Morphology and electromechanical properties of RGO-VY

To confirm the presence of GO on yarn, the XPS images have been provided (Fig. 3) and the results are summarized in Table 1. As shown in Table 1, the C–O% of viscose fabric, GO and GO coated

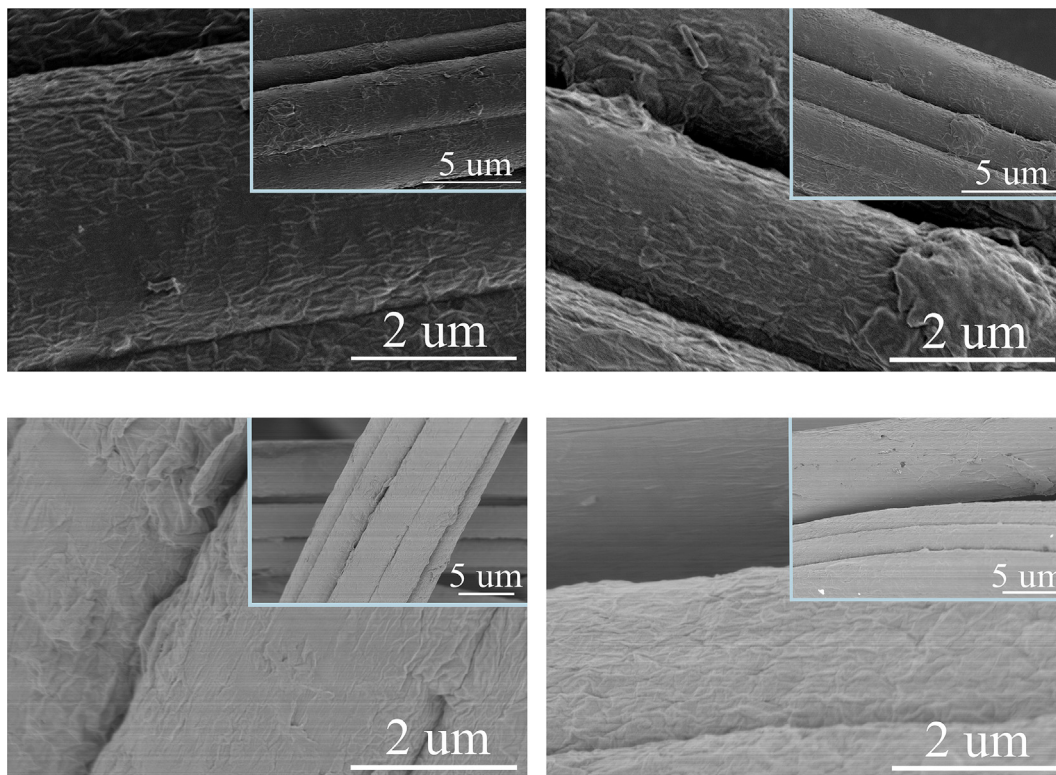


Fig. 4. SEM images of original RGO-VY (A) and RGO-VY after the drawing treatment at different strain rate of 15% (B), 30% (C) and 45% (D). (A colour version of this figure can be viewed online.)

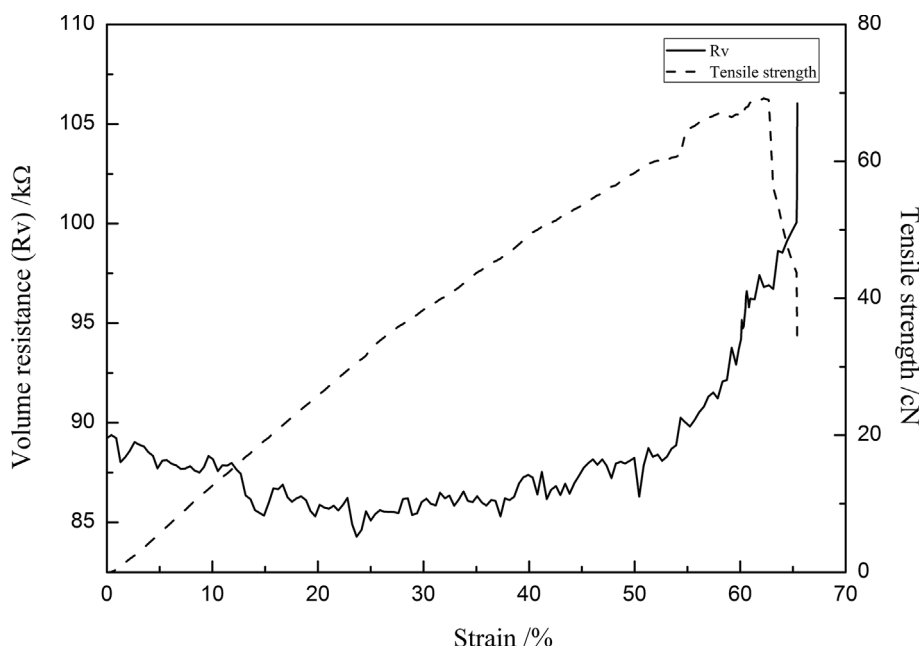


Fig. 5. Tensile strength and resistance of RGO-VY under strain.

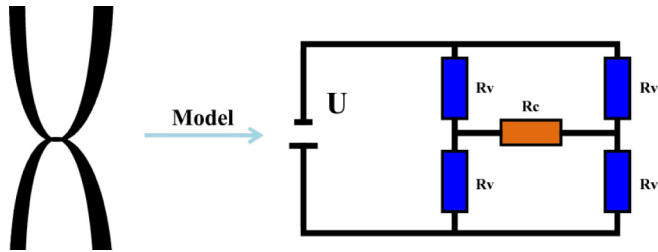


Fig. 6. The model of hook yarn. (A colour version of this figure can be viewed online.)

$$R^* = \begin{bmatrix} 2Rv + Rc & -Rc & -Rv \\ -Rc & 2Rv + Rc & -Rv \\ -Rv & -Rv & 2Rv \end{bmatrix} \quad (7)$$

$$Rc = \sqrt{29.25Rv^2 - \frac{R}{Rv}} \quad (8)$$

viscose fabric were 43.62%, 6.61% and 36.91% respectively, and meantime, the C=O % of viscose fabric, GO and GO coated viscose fabric were 13.11%, 47.59% and 16.85% respectively. The decrease of C–O% and increase of C=O % of GO coated viscose fabric compared with that of viscose fabric both suggests attachment of the GO onto the surface of viscose fabric.

Fig. 4 shows the surface of RGO-VY before and after the drawing treatment at strain rates of 15%, 30% and 45%. As shown in Fig. 4A, it was observed that viscose yarns were uniformly coated into RGO films. After the drawing treatment, the morphology of RGO films was not obviously changed at strain rate of 15% and 30%. However, under further drawing, RGO layers on the surface of yarns slipped and the packing structure between layers became loose at strain rate of 45%, resulting in the decrease of contacting area among RGO layers or between RGO layers and viscose yarns (Seen from Fig. 4B–D). Some researchers have reported that RGO can adhere to the fabrics through strong hydrogen interactions, causing the

stability of assembly structure of RGO layers [28,29].

Strain-tensile strength and strain-resistance curves of RGO-VY yarns are shown in Fig. 5. The initial resistance value of RGO-VY was 89.22 kΩ. At a strain rate of 23.67%, the resistance became slightly decreased to 84.28 kΩ. With further strain, the resistance of RGO-VY sharply increased to 96.81 kΩ at the maximum strain value of 62.25%. The results demonstrate that before the onset of material failure, the resistance exhibited an initial decline followed by an ascent.

According to Fig. 1, the unit loop of knitted fabrics was composed of four hook points and five line segments, and the simulated model of each hook is illustrated in Fig. 6. The closed circuit is comprised of four volume resistors and one contacting resistor. According to Kirchhoff's law, R^* is given by Eq (7) and the calculation of Rc follows in Eq (8). Strain-tensile strength and strain-resistance curves of RGO-VY knitted fabrics are plotted in Fig. 7.

Initially upon strain the hook resistance R retained an average value of 27.32 ± 0.63 kΩ. At 39.33% strain, R increased sharply to a maximum value of 76.94 kΩ. The resulting contacting resistance, Rc , had an initial value of 281.78 kΩ, and decreased with strain. At 25.88% strain, $Rc = 266.18$ kΩ. With further strain, Rc rose slightly. Upon yarn fracturing, $Rc = 271.84$ kΩ, which was still smaller than the initial value. These results provide experimental verification for the theoretical analysis of the fabric resistance.

3.2. Electromechanical properties of conductive yarns assembles

The resistance of the fabrics could be simulated and compared to experimental data (Figs. 8 and 9).

When knitted fabrics were drawn under transverse direction (Fig. 8A), the experimental value of the resistance slightly decreased from 8.75 kΩ to a minimum of 8.42 kΩ. At higher strain, the resistance increased up to 12.96 kΩ, at which point the strain was 160.23% and the fabric fractured. During longitudinal drawing of fabrics (Fig. 8B), the resistance increased from 11.98 kΩ to 15.34 kΩ, when the fabrics fractured (at a strain of 149.451%). The woven fabrics exhibited a similar tendency under diagonal strain as compared with the longitudinal drawing of knitted fabrics, and the resistance changed from 0.96 kΩ to 1.66 kΩ until the fracture of the

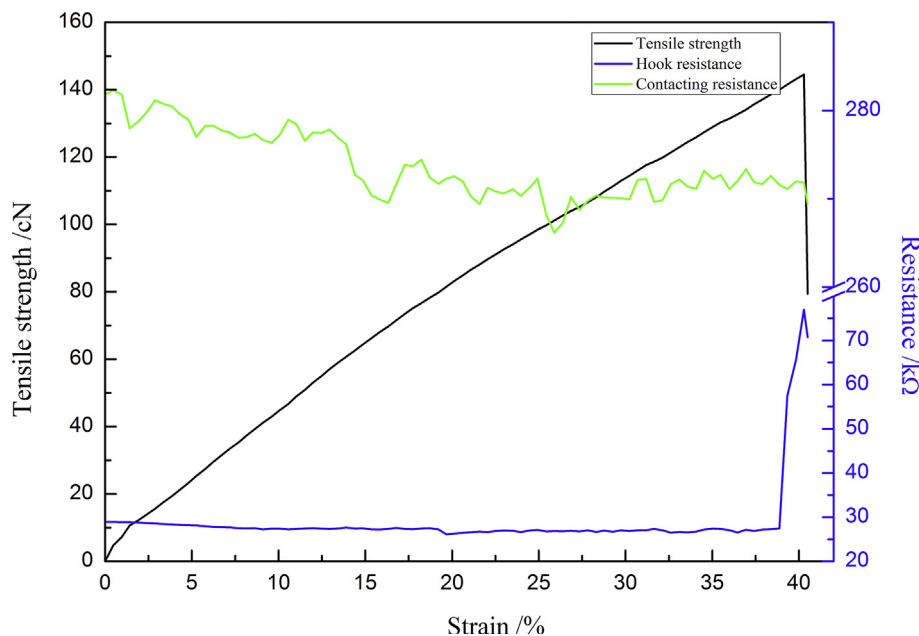


Fig. 7. R and Rc of hook site under strain. (A colour version of this figure can be viewed online.)

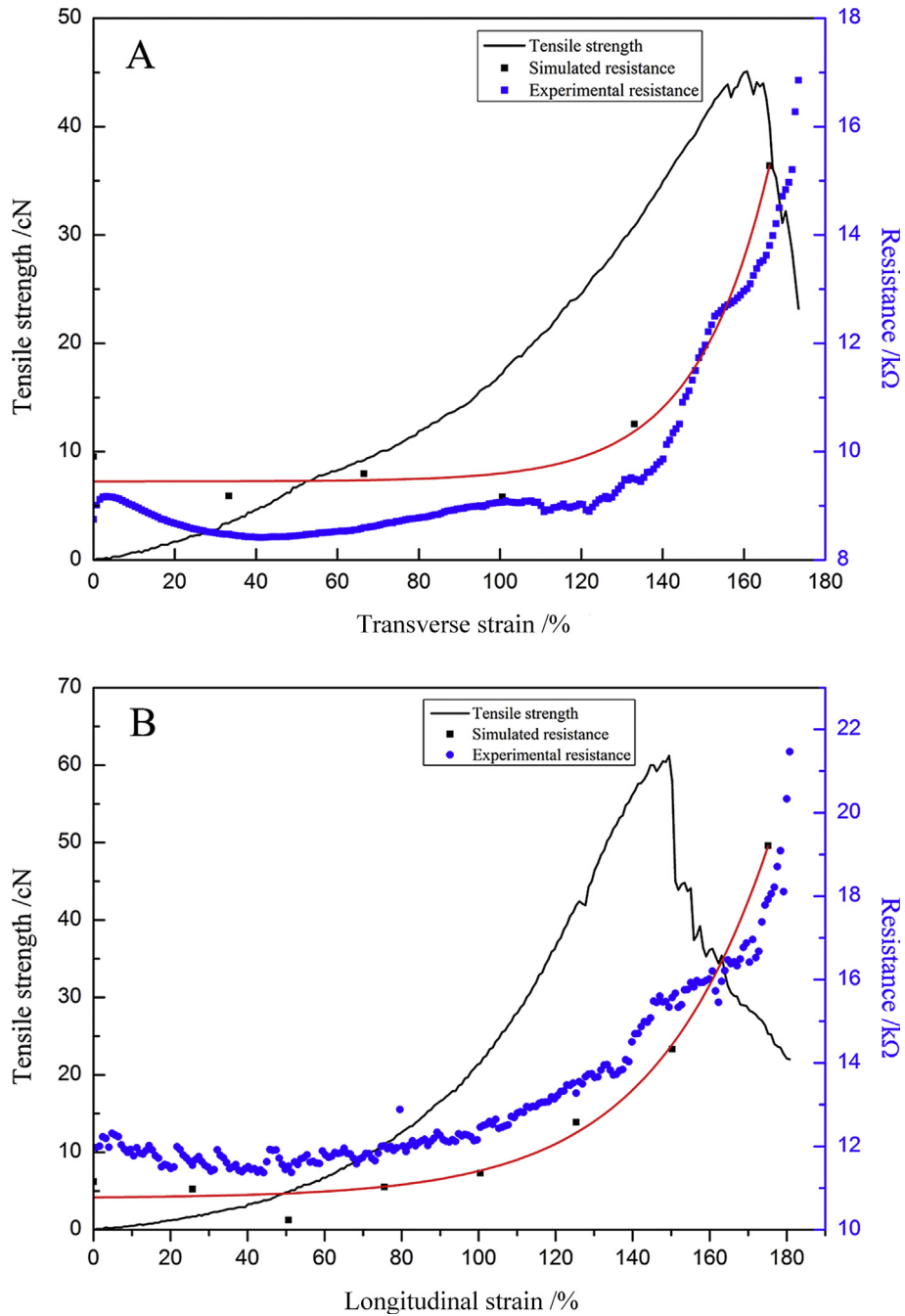


Fig. 8. Simulated and experimental results of knitted fabrics under transverse (A) and longitudinal strain (B). (A colour version of this figure can be viewed online.)

fabric as shown in Fig. 9.

The simulated results agreed reasonably with the experimental data (Figs. 8 and 9). The major trends of both simulated and experimental data were consistent but had certain errors, which may be caused by several reasons. (1) The fabrics were treated as whole conductors in the simulation process, while in reality they were composed of many fibers. (2) In the simulation process, the hook sites and hook resistance were treated as static. In fact, during strain of the knitted fabric, the hook sites slid relative to one another and the resistance was dynamic. (3) The loops of knitted fabrics and warp and weft of woven fabrics were treated as two-dimensional plane models, when in fact the stitch structure occupies a three-dimensional spatial model and the yarn segments

were curved. (4) The fitting results of woven fabrics were poorer than those of knitted fabrics; this was mainly due to the fact that the angle of warp and weft was assumed to be constant when in actuality it will deform upon strain. In addition, the contacting resistance in woven model was ignored due to high complexity in the calculation.

3.3. Deformation analysis of drawing fabrics

Fig. 10 shows the change of stitch structure of knitted fabrics during strain. During transverse strain, loops were observed to flatten, while during longitudinal strain the loops were found to strain until they became lanky. A similar work by Wu et al.

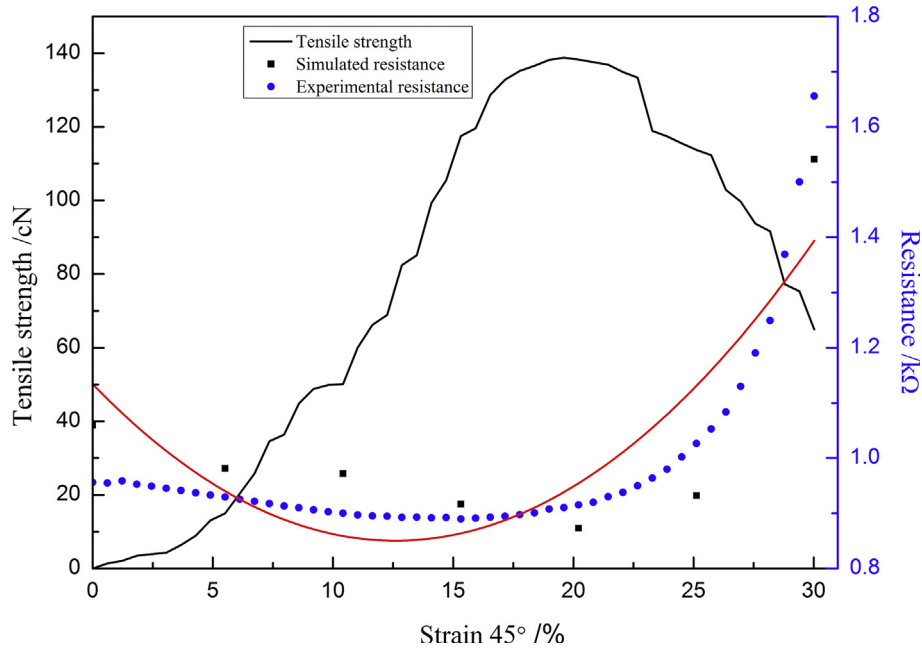


Fig. 9. Simulated and experimental results of weave fabrics under diagonal strain. (A colour version of this figure can be viewed online.)

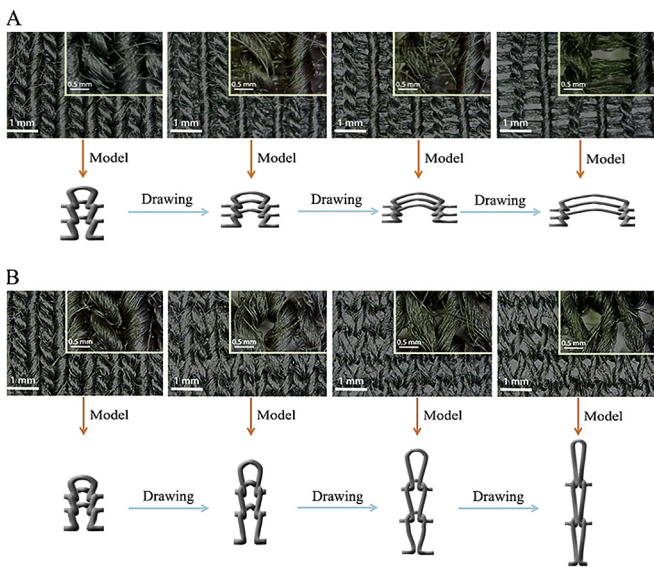


Fig. 10. Change of stitch structure of knitted fabrics in the drawing process. (A colour version of this figure can be viewed online.)

explained the computer simulation method for predicting the deformation behavior of fundamental weft-knitted fabrics [30].

For both tensile processes, the morphology of yarn segments changed from curved to linear with strain. Upon further drawing the yarns became attenuated, resulting in a decrease of transfer rate of electrons [31]. In the hook points, due to the increased strain, the contacting area of yarns increased, accelerating the movement of electrons [32]. It was concluded that the electrical properties of conductive fabrics could be controlled by changing the characteristics of yarns or the stitch structure of loops with different sizes and/or tightness.

During strain of woven fabrics (Fig. 11), while drawing in a diagonal direction, the migration of warp and weft was observed and the stitch density increased. When the fabrics were further drawn, the fibers squeezed together and flattened, and finally the warp and weft fibers formed an integrated whole with no observable gaps. This process could change the contact area from point-to-point to line-to-line and finally to face-to-face, resulting in an increase of motion space of electrons and an improvement in transfer rate [25]. Thus, controlling the density of warp and weft is key to controlling electrical properties when designing conducting woven fabrics. In particular, fabrics with high densities exhibited smaller resistivity.

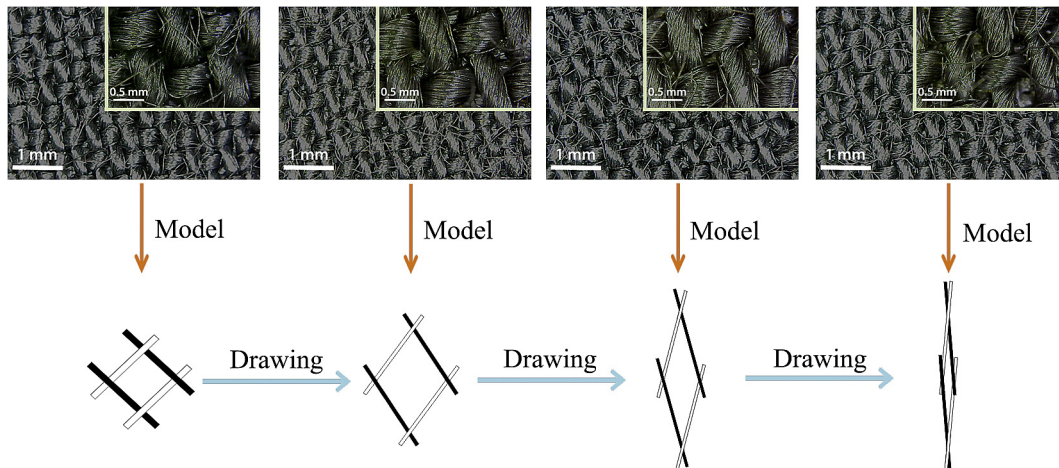


Fig. 11. Change of stitch structure of weave fabrics in the drawing process. (A colour version of this figure can be viewed online.)

4. Conclusions

In our work, conductive viscose yarns were prepared through the coating of graphene oxide and reduction of hydrazine hydrate, and after that, knitted and woven fabrics could be obtained. Based on the R_v and R_c of yarns and models of both fabric types, simulation results of equivalent resistance of both fabrics could be obtained. These agreed reasonably with the experimental data and major trends of both results were consistent. In addition, when knitted fabrics were drawn, the morphology of yarn segments changed from curved to linear, and with further drawing, the yarns became attenuated, resulting in a decrease in transfer rate of electrons. For the hook points of knitted fabrics, the contacting area between yarns was elevated during strain, accelerating the movement of electrons. The fibers of the woven fabrics were squeezed together and flattened when the fabrics were drawn until finally the warp and weft yarns formed an integrated whole. This was found to change the fiber contacts from point-to-point to line-to-line and finally face-to-face, resulting in an increase of motion space of electrons and improvement of transfer rate. The findings presented here provide a fundamental guide to help the design of flexible conductive fabrics with controllable electromechanical properties.

Acknowledgments

The financial support from the scholarship of key laboratory of yarn material forming and processing technology of Zhejiang Province (MTC 2014-002), Jiaying project of innovation team (MTC 2015-001, MTC 2015-005 and MTC 2015-008) and the financial support from scientific research project of Jiaying university (70515005) is also acknowledged. All authors thank Dr. Camelia Stan for proofreading this manuscript.

References

- [1] A. Ramadoss, B. Saravanakumar, J.K. Sang, Thermally reduced graphene oxide-coated fabrics for flexible supercapacitors and self-powered systems, *Nano Energy* 15 (0) (2015) 587–597.
- [2] C. Zhao, K. Shu, C. Wang, S. Gambhir, G.G. Wallace, Reduced graphene oxide and polypyrrole/reduced graphene oxide composite coated stretchable fabric electrodes for supercapacitor application, *Electrochim. Acta* 172 (0) (2015) 12–19.
- [3] J. Molina, J. Fernández, J.C. Inés, A.I. Río, J. Bonastre, F. Cases, Electrochemical characterization of reduced graphene oxide-coated polyester fabrics, *Electrochim. Acta* 93 (4) (2013) 44–52.
- [4] Q. Zhou, X. Ye, Z. Wan, C. Jia, A three-dimensional flexible supercapacitor with enhanced performance based on lightweight, conductive graphene-cotton fabric electrode, *J. Power Sources* 296 (0) (2015) 186–196.
- [5] X. Pu, L. Li, M. Liu, C. Jiang, C. Du, Z. Zhao, et al., Wearable self-charging power textile based on flexible yarn supercapacitors and fabric nanogenerators, *Adv. Mater.* 28 (1) (2016) 98–105.
- [6] W. Zeng, L. Shu, Q. Li, S. Chen, F. Wang, X.M. Tao, Fiber-based wearable electronics: a review of materials, fabrication, devices and applications, *Adv. Mater.* 26 (31) (2014) 5310–5336.
- [7] F. Meng, R. Li, Q. Li, W. Lu, T.W. Chou, Synthesis and failure behavior of super-aligned carbon nanotube film wrapped graphene fibers, *Carbon* 72 (72) (2014) 250–256.
- [8] X. Ji, Y. Xu, W. Zhang, L. Cui, J. Liu, Review of functionalization, structure and properties of graphene/polymer composite fibers, *Compos. Part A* 87 (0) (2016) 29–45.
- [9] Z. Gao, C. Bumgardner, N. Song, Y. Zhang, J. Li, X. Li, Cotton-textile-enabled flexible self-sustaining power packs via roll-to-roll fabrication, *Nat. Commun.* 7 (0) (2015) 11586.
- [10] B. Vigolo, A. Pénicaud, C. Coulon, C. Sauder, R. Pailler, C. Journet, et al., Macroscopic fibers and ribbons of oriented carbon nanotubes, *Science* 290 (5495) (2000) 1331–1334.
- [11] J. Ci, N. Punbusayakul, J. Wei, R. Vajtai, S. Talapatra, P.M. Ajayan, Multifunctional macro architectures of double-walled carbon nanotube fibers, *Adv. Mater.* 19 (13) (2007) 1719–1723.
- [12] Z. Xu, C. Gao, Graphene chiral liquid crystals and macroscopic assembled fibres, *Nat. Commun.* 2 (0) (2011) 571.
- [13] L. Bao, J. Zang, X. Li, Flexible Zn_2SnO_4/MnO_2 core/shell nanocable-carbon microfiber hybrid composites for high-performance supercapacitor electrodes, *Nano Lett.* 11 (3) (2011) 1215–1220.
- [14] L. Bao, X. Li, Towards textile energy storage from cotton T-shirts, *Adv. Mater.* 24 (24) (2012) 3246–3252.
- [15] X. Tang, M. Tian, L. Qu, S. Zhu, X. Guo, G. Han, et al., Functionalization of cotton fabric with graphene oxide nanosheet and polyaniline for conductive and UV blocking properties, *Synth. Met.* 202 (0) (2015) 82–88.
- [16] Z. Gao, N. Song, Y. Zhang, X. Li, Cotton-textile-enabled, flexible lithium-ion batteries with enhanced capacity and extended lifespan, *Nano Lett.* 15 (12) (2015) 8194–8203.
- [17] Z. Gao, N. Song, X. Li, Microstructural design of hybrid $CoO@NiO$ and graphene nano-architectures for flexible high performance supercapacitors, *J. Mater. Chem. A* 3 (28) (2015) 14833–14844.
- [18] Z. Gao, W. Yang, J. Wang, N. Song, X. Li, Flexible all-solid-state hierarchical $NiCo_2O_4$ /porous graphene paper asymmetric supercapacitors with an exceptional combination of electrochemical properties, *Nano Energy* 13 (0) (2015) 306–317.
- [19] Z. Gao, N. Song, Y. Zhang, X. Li, Cotton textile enabled, all-solid-state flexible supercapacitors, *RSC Adv.* 5 (20) (2015) 15438–15447.
- [20] H. Zhang, X. Tao, T. Yu, S. Wang, Conductive knitted fabric as large-strain gauge under high temperature, *Sens. Actuators A* 126 (1) (2006) 129–140.
- [21] V. Narayanunni, H. Gu, C. Yu, Monte Carlo simulation for investigating influence of junction and nanofiber properties on electrical conductivity of segregated-network nanocomposites, *Acta Mater.* 59 (11) (2011) 4548–4555.
- [22] H. Yu, D. Heider, S.A. Advani, 3D microstructure based resistor network model for the electrical resistivity of unidirectional carbon composites, *Compos Struct.* 134 (0) (2015) 740–749.
- [23] C. Ganser, P. Kreiml, R. Morak, F. Weber, O. Paris, R. Schennach, et al., The effects of water uptake on mechanical properties of viscose fibers, *Cellulose* 22 (4) (2015) 2777–2786.
- [24] S.Y. Cho, Quantum kirchhoff's current law and spin current in mesoscopic electronics, *J. Korean Phys. Soc.* 58 (5) (2011) 1151–1155.
- [25] X. Tao, *Wearable Electronics and Photonics*, Woodhead Publishing, Hongkong, 2005, pp. 81–102.
- [26] W.S. Hummers, R.E. Offeman, Preparation of graphitic oxide, *J. Am. Chem. Soc.* 80 (6) (1958) 1339.
- [27] C. Zhao, K. Shu, C. Wang, S. Gambhir, G.G. Wallace, Reduced graphene oxide and polypyrrole/reduced graphene oxide composite coated stretchable fabric electrodes for supercapacitor application, *Electrochim. Acta* 172 (0) (2015) 12–19.
- [28] I.A. Sahito, K.C. Sun, A.A. Arbab, M.B. Qadir, S.H. Jeong, Graphene coated cotton fabric as textile structured counter electrode for DSSC, *Electrochim. Acta* 173 (0) (2015) 164–171.
- [29] L. Gan, S. Shang, C.W.M. Yuen, S. Jiang, Graphene nanoribbon coated flexible and conductive cotton fabric, *Compos Sci. Technol.* 117 (2) (2015) 208–214.
- [30] W.L. Wu, H. Hamada, Z. Maekawa, Computer simulation of the deformation of weft-knitted fabrics for composite materials, *J. Text. Inst.* 85 (2) (1994) 198–214.
- [31] P. Xue, X.M. Tao, K.W.Y. Kwok, M.Y. Leung, Electromechanical behavior of fibers coated with an electrically conductive polymer, *Text. Res. J.* 74 (10) (2004) 929–936.
- [32] K.W. Oh, H.J. Park, S.H. Kim, Stretchable conductive fabric for electrotherapy, *J. Appl. Polym. Sci.* 88 (5) (2003) 1225–1229.